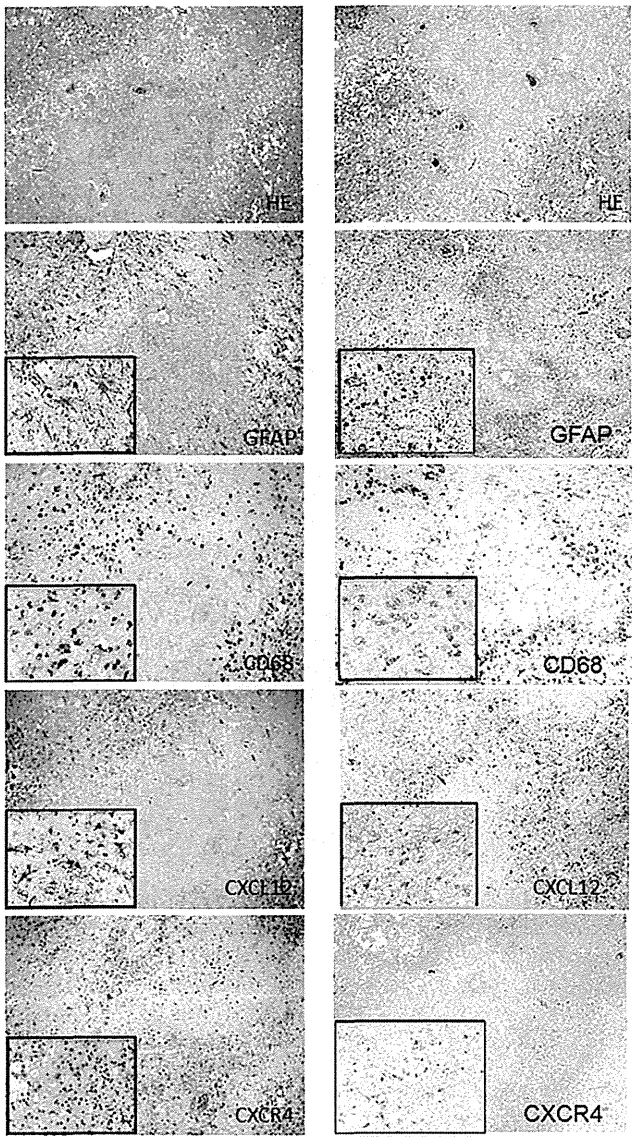

Figure 2. H&E staining and immunohistochemistry for GFAP, CD68, CXCL12 and CXCR4 of the surgical specimen from Case 2 in the left column and for Case 3 in the right column. H&E staining showed the necrotic core and the surrounding tissue (perinecrotic area). Immunohistochemical staining for GFAP, CD68, CXCL12 and CXCR4 revealed GFAP- and CXCL12-positive astrocytic cells, and CD68- and CXCR4-positive oval cells in the perinecrotic area. CD68- and CXCR4-positive cells were also observed in small numbers inside the necrotic core. On the other hand, no or scarce immunoreactivity of GFAP and CXCL12 was observed in the necrotic core. The original objective magnifications were ×40 and ×200.

core, though to a lesser degree. We then examined the expression of NF-κB as a master molecule of inflammation in RN using the Case 2 specimens. Interestingly, NF-κB was expressed not in normal brain tissue but in the perinecrotic area (Fig. *s*1). This molecule was expressed not only in the cytoplasm but also in the nucleus, and was morphologically assessed as a monocyte. The same tendency was confirmed in Case 3.

Subsequently, we focused on immune cells in the brain to determine their effect on RN. To this end, we performed an immunohistochemical study using hGLUT5, CD68 and CD45 antibodies, as stated above. We observed similar distributions in hGLUT5-positive cells and CD68-positive cells in Cases 3 and 4 (Fig. *s*2). However, the number of CD45-positive cells was limited; their distribution pattern was distinguishable from those of GFAP-positive cells and CD68- and hGLUT5-positive cells. The same tendencies were observed in Cases 6 and 7 (data not shown).

Taken together, these data suggested that CXCL12 and CXCR4 might be expressed in GFAP-positive reactive astrocytes and hGLUT5- and/or CD68-positive cells, respectively. Also, microglias, macrophages, and even lymphocytes, each of which can produce proinflammatory cytokines, accumulated in the perinecrotic area. Therefore, inflammation might play a significant role in the pathogenesis of RN in the brain.

Relationships between CXCL12, CXCR4, HIF-1α, VEGF, IL-1α, IL-6 and TNF-α expression and GFAP/CD68 expression in radiation necrosis

In order to further examine the distribution of cells responsible for the expression of cytokines and chemokines, we performed double immunofluorescence staining. The specimen from Case 2 provided a representative pattern (Figs 3 and 4). Figure 3 shows that the expression of HIF-1α was recognized not in GFAP-positive cells (a) but in most CD68-positive cells (b). However, some CD68-positive cells did not produce HIF-1α, while some CD68-negative cells did. VEGF was expressed in GFAP-positive cells (c) but was hardly expressed in CD68-positive cells (d). Likewise, the expression of CXCL12 was detected in GFAP-positive cells (e) but not in CD68-positive cells (f). In contrast, CXCR4 was not expressed in GFAP-positive cells (g) but was expressed in CD68-positive cells (h). However, some CXCR4 expression was recognized in CD68-negative cells.

Furthermore, Fig. 4 shows that IL-1α, IL-6 and TNF-α were not expressed in GFAP-positive cells (a, c, e) but were expressed in CD68-positive cells (b, d, f). The same tendencies were confirmed in the other specimens (data not shown).

Relationships between CXCR4, HIF-1α and IL-1α expression and hGLUT5/CD68 and CD45 expression in radiation necrosis

In order to identify the cells that are responsible for inflammation in RN, we analyzed double immunofluorescence using anti-CD68, anti-hGLUT5 and anti-CD45 antibodies. We used the former two antibodies to distinguish microglias from macrophages originating from peripheral blood in CD68-positive cells. Figure *s*3 (Case 1) shows that CXCR4, HIF-1α and IL-1α were expressed in many hGLUT5-positive cells (a, b, c). However, some CXCR4, HIF-1α and IL-1α-positive cells did not express hGLUT5 and vice versa. Also, most CD68-positive cells were identical to hGLUT5-positive cells,

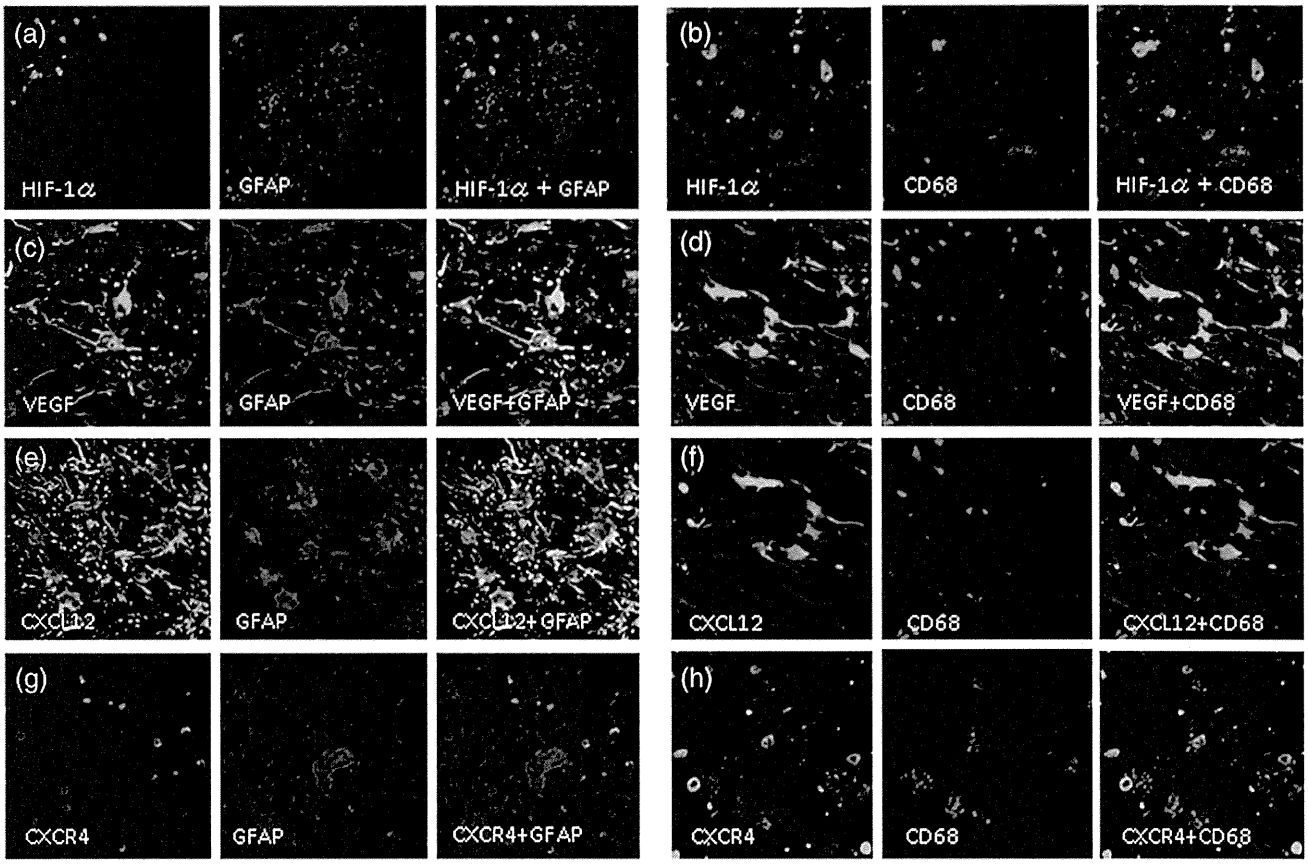

Figure 3. Double immunofluorescence staining of the specimen from Case 2. The expression of HIF-1α was not detected in reactive astrocytes, as revealed by GFAP (**a**), but was detected in CD68-positive cells (**b**). VEGF was expressed in GFAP-positive cells (**c**) but was hardly expressed in CD68-positive cells (**d**). Similarly, CXCL12 was expressed in GFAP-positive reactive astrocytes (**e**) but not in CD68-positive cells (**f**). In contrast, CXCR4 was not expressed in GFAP-positive cells (**g**) but was expressed in CD68-positive cells (**h**). The original objective magnification was ×400.

although some cells expressed only CD68 or hGLUT5 (d). Almost no CD45-positive cells produced IL-1α. Interestingly, almost all CD45-positive cells co-expressed CXCR4 (data not shown). This is confirmed in the other cases.

DISCUSSION

Medical treatment with the anti-VEGF antibody BV, or surgical resection of necrotic tissue containing VEGF-producing cells may serve to decrease perilesional edema and immediately improve symptoms stemming from the efficient reduction of VEGF in the perinecrotic area [1–3, 5]. These phenomena suggest that VEGF is the key molecule in the pathogenesis of RN. Here the role of reactive astrocytes in RN is clearly the production of VEGF, while that of monocytes remains unclear. The present results prove that these monocytes in the perinecrotic area produce HIF-1α. HIF-1α is a well-known transactivator not only for VEGF, but also for the CXCL12-CXCR4 axis [6, 7, 16]. The CXCL12-CXCR4 axis is also well known to be a chemotactic factor and to play a significant role in inflammation. Therefore, we examined the expression of these molecules in RN. As we had speculated, CXCR4-positive monocytes and lymphocytes gathered in the perinecrotic area.

Yoshii *et al.* stressed the mechanism underlying the development and progress of late cerebral RN, with special emphasis on inflammatory responses [8]. They put forward the following hypothesis to explain the mechanism underlying RN. First, irradiation damages endothelial cells, causing the blood–brain barrier (BBB) to fail. The inflammatory cells then cross into the extravascular space. At the same time, these cells secrete cytokines that cause other inflammatory cells to develop. This effect becomes an uncontrolled inflammatory response and continues, becoming chronic inflammation [8]. Thereafter we examined the role of inflammation in RN more precisely by using immunohistochemistry and double immunofluorescence. Kureshi *et al.* reported that macrophages and some astrocytes might migrate to the RN area and produce IL-1α, TNF-α and IL-6 [17]; this would be partly consistent with our present results, although the exact cell types corresponding to each type of cytokine production were ambiguous in their report. In laboratory animal RN

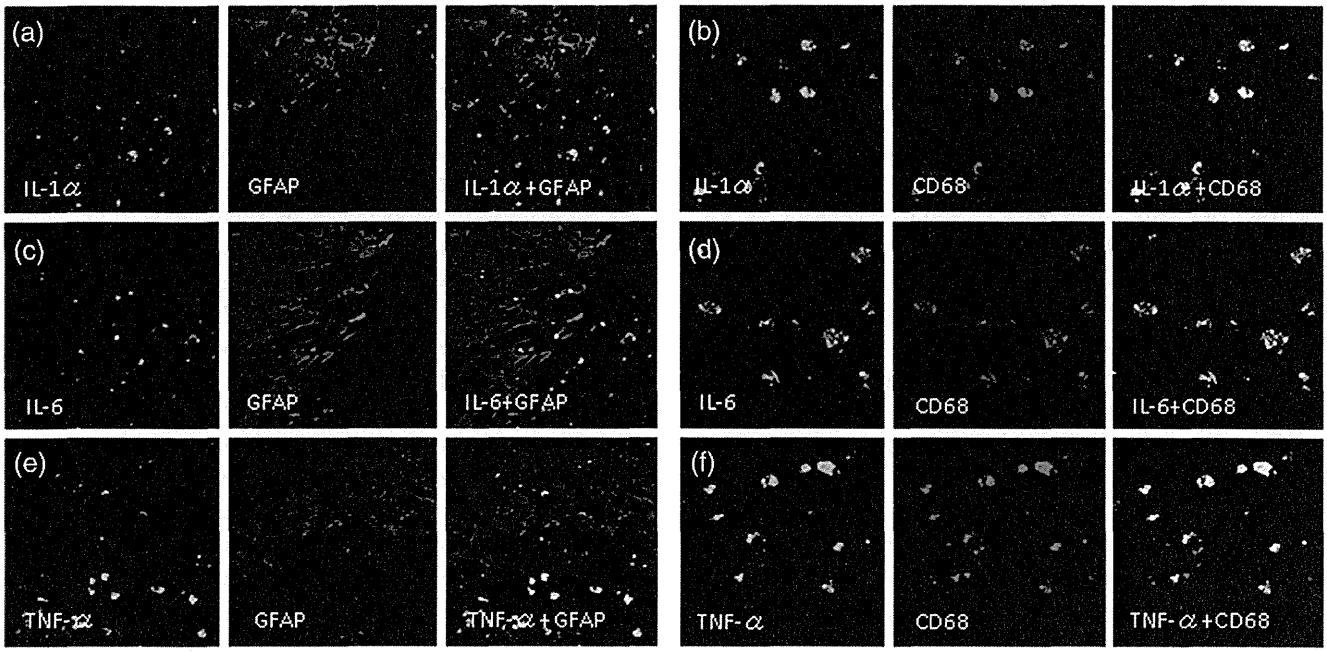

Figure 4. Double immunofluorescence staining of Case 2. IL-1α, IL-6 and TNF-α were not expressed in reactive astrocytes, as revealed by GFAP-positive cells (**a**, **c**, **e**), but were expressed in CD68-positive cells (**b**, **d**, **f**). The original objective magnification was ×400.

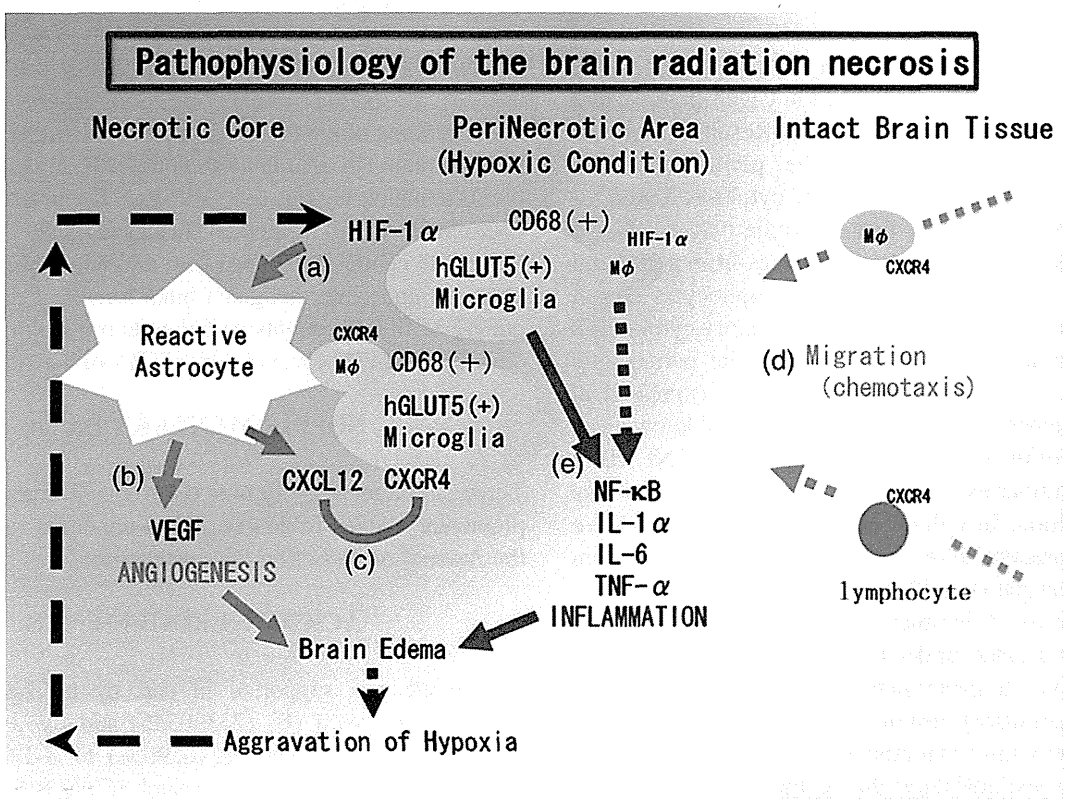

Figure 5. Hypothesis of the pathophysiology of brain radiation necrosis. (**a**) Vascular damage around the irradiated tumor tissue caused tissue ischemia. This hypoxia induced hGLUT5-positive microglias to express HIF-1α around the necrotic core. (**b**) Under HIF-1α regulation, VEGF was expressed in reactive astrocytes, causing leaky and fragile angiogenesis. (**c**) CXCL12/CXCR4 signaling is also regulated by HIF-1α. (**d**) CXCL12-expressing reactive astrocytes might draw CXCR4-expressing macrophages and lymphocytes by chemotaxis into the perinecrotic area. (**e**) These accumulated hGLUT5-positive microglias producing NF-κβ and pro-inflammatory cytokines seemed to aggravate radiation necrosis.

models, a key cytokine is TNF-α, which regulates other pro-inflammatory cytokines to increase BBB permeability and leukocyte adhesion, to activate astrocytes, and to induce endothelial apoptosis [18–21]. Moreover, IL-1α, either alone or in cooperation with TNF-α and IL-6 in the downstream region, exacerbates inflammation [22].

The roles of chemokine CXCL12 and its receptor CXCR4 have been well established in the immune and nervous systems, where they localize in various cell types with specific microenvironments [23]. CXCR4 is expressed not only in monocytes, but also in lymphocytes [24, 25]. In the present study, CD45-positive cells expressed CXCR4, as described in Results. Thereafter, these lymphocytes might be drawn into the perinecrotic area from peripheral blood by homing; however, unlike CD68- and/or hGLUT5-positive cells, they did not produce pro-inflammatory cytokines. At first, in this study, we used CD68 antibody to detect monocytes. But it was difficult for us to discriminate microglia from a macrophage in brain tissue using only this marker. Horikoshi and Sasaki *et al.* reported that the hGLUT5 antibody is a good and specific marker for microglia [26–32]. We therefore used it to recognize microglia. In the present study, CD68 and hGLUT5 were usually expressed in many identical cells, although some hGLUT5-positive cells did not show CD68 expression and vice versa. HIF-1α, CXCR4 and IL-1α expression was confined largely to hGLUT5-positive cells, but some of them were expressed in CD68-positive and hGLUT-5–negative cells, as stated in Results. Also, as described above, CD45 cells in the perinecrotic area expressed CXCR4 but not inflammatory cytokine. Taken together, these findings suggest that microglia play a key role in this inflammation, but some macrophages from peripheral blood may also be involved. However, lymphocytes do not participate in the production of pro-inflammatory cytokines.

We also examined NF-κB expression in the perinecrotic area (Fig. *s*1). At a glance, this molecule was expressed in monocytes in the perinecrotic area. NF-κB is well known as a major molecule of inflammation. As the function of NF-κB in RN is unclear, further examination is needed to elucidate this molecule's function. In culture conditions, CXCR4-positive microglia can produce IL-6 with CXCL12 stimuli via an NF-κB-dependent pathway [33]. This may suggest a role of NF-κB in RN. Also, it is observed in cerebral ischemia that CXCL12 is upregulated under ischemic conditions, thereby inducing monocytes to gather in the ischemic penumbra and a subsequent inflammatory response [34–36]. These observations support chemokine–cytokine interaction in RN.

From the observed qualitative data in this study, let us summarize our original hypothesis about RN pathophysiology (Fig. 5). That is, the first step in a brain undergoing radiation therapy and developing necrosis is blood vessel damage just around the tumor. This is connected with hypoxia close to the irradiated tumor tissue, which causes the upregulation of HIF-1α in hGLUT5-positive microglias. Because HIF-1α is well known as a transactivator of VEGF and CXCL12/CXCR4 signaling [7, 16], the upregulation of HIF-1α augments VEGF and CXCL12 expression in GFAP-positive reactive astrocytes. The former produced the leaky and fragile angiogenesis and the subsequent perilesional edema in RN. The latter might draw CXCR4-expressing hGLUT5-positive microglias and CXCR4-expressing lymphocytes by chemotaxis to the perinecrotic area. The production of pro-inflammatory cytokines by these accumulated hGLUT5-positive cells seemed to aggravate the perilesional edema. However, although some CD45-positive lymphocytes gathered in the perinecrotic area, they were not involved in pro-inflammatory cytokine production. NF-κB must play a significant role in RN inflammation. The aggravation of edema could lead to the further development of focal ischemia, which augments the expression of HIF-1α in the microglias in the perinecrotic area. Here, both angiogenesis and inflammation may contribute to a synergistic and malignant RN cycle. These hypotheses need to be confirmed in experimental animal models, as described below. In any case, the present results suggest that inflammation participates in the pathophysiology of brain RN.

The present research appears to have elucidated a part of the molecular mechanism underlying brain RN on the basis of qualitative histology and immunohistochemistry. In order to prove these hypotheses more conclusively, it will be necessary to create a brain RN model in laboratory animals and to analyze the pathophysiology in each stage. An improved understanding of the mechanism by which the numerous cytokines in brain RN are regulated could play an important role in the formulation of treatment strategies. If a brain RN becomes controllable, it will further advance the application of radiation therapy to central nervous system tumors, leading to the conquest of intractable malignant brain tumors. Furthermore, the quality of life of patients would certainly be improved by an effective treatment for symptomatic RN of the brain.

SUPPLEMENTARY DATA

Three supplementary figures (Figs *s*1, *s2* and *s3*), one supplementary table (Table *s*1), and an appendix are available at the *Journal of Radiation Research* online.

ACKNOWLEDGEMENTS

This work was supported in part by a Grant-in-Aid for Scientific Research (B) (23390355) and by a Grant-in-Aid for Exploratory Research (24659658) to S-I.M., and by a Grant-in-Aid for Scientific Research (C) (23592145) to M.F. from the Japanese Ministry of Education, Culture, Sports, Science, and Technology. We thank Itsuko Inoue, Kaname Shimokawa and Shizuka Akashi for their technical assistance. We also thank Prof. Kazuhito Tomizawa (Department of Molecular Physiology, Kumamoto University), Dr Mitsugu Fujita (Department of Microbiology and Neurosurgery, Kinki

University Graduate School of Medical Sciences) and Dr Satoshi Kokura (Department of Molecular Gastroenterology and Hepatology, Kyoto Prefectural University of Medicine) for their critical reading and fruitful discussions concerning this manuscript.

FUNDING

Funding to pay Open Access publication charges for this article was provided by a Grant-in-Aid for Scientific Research (B) (23390355) and by a Grant-in-Aid for Exploratory Research (24659658) to S-I.M., and by a Grant-in-Aid for Scientific Research (C) (23592145) to M.F. from the Japanese Ministry of Education, Culture, Sports, Science, and Technology.

REFERENCES

1. Furuse M, Kawabata S, Kuroiwa T *et al.* Repeated treatments with bevacizumab for recurrent radiation necrosis in patients with malignant brain tumors: a report of 2 cases. *J Neurooncol* 2011;**102**:471–5.
2. Gonzalez J, Kumar AJ, Conrad CA *et al.* Effect of bevacizumab on radiation necrosis of the brain. *Int J Radiat Oncol Biol Phys* 2007;**67**:323–6.
3. Levin VA, Bidaut L, Hou P *et al.* Randomized double-blind placebo-controlled trial of bevacizumab therapy for radiation necrosis of the central nervous system. *Int J Radiat Oncol Biol Phys* 2011;**79**:1487–95.
4. Nonoguchi N, Miyatake S, Fukumoto M *et al.* The distribution of vascular endothelial growth factor-producing cells in clinical radiation necrosis of the brain: pathological consideration of their potential roles. *J Neurooncol* 2011;**105**:423–31.
5. Miyatake S, Kuroiwa T, Kajimoto Y *et al.* Fluorescence of non-neoplastic, magnetic resonance imaging-enhancing tissue by 5-aminolevulinic acid: case report. *Neurosurgery* 2007;**61**: E1101–3; discussion E1103–4.
6. Kryczek I, Wei S, Keller E *et al.* Stroma-derived factor (SDF-1/CXCL12) and human tumor pathogenesis. *Am J Physiol Cell Physiol* 2007;**292**:C987–95.
7. Liang Z, Brooks J, Willard M *et al.* CXCR4/CXCL12 axis promotes VEGF-mediated tumor angiogenesis through Akt signaling pathway. *Biochem Biophys Res Commun* 2007;**359**:716–22.
8. Yoshii Y. Pathological review of late cerebral radionecrosis. *Brain Tumor Pathol* 2008;**25**:51–8.
9. Kawabata S, Miyatake S, Kuroiwa T *et al.* Boron neutron capture therapy for newly diagnosed glioblastoma. *J Radiat Res* 2009;**50**:51–60.
10. Miyatake S, Kawabata S, Kajimoto Y *et al.* Modified boron neutron capture therapy for malignant gliomas performed using epithermal neutron and two boron compounds with different accumulation mechanisms: an efficacy study based on findings on neuroimages. *J Neurosurg* 2005;**103**:1000–9.
11. Miyatake S, Kawabata S, Nonoguchi N *et al.* Pseudoprogression in boron neutron capture therapy for malignant gliomas and meningiomas. *Neuro-Oncology* 2009;**11**:430–6.
12. Miyatake S, Kawabata S, Yokoyama K *et al.* Survival benefit of Boron neutron capture therapy for recurrent malignant gliomas. *J Neurooncol* 2009;**91**:199–206.
13. Miyatake S, Tamura Y, Kawabata S *et al.* Boron neutron capture therapy for malignant tumors related to meningiomas. *Neurosurgery* 2007;**61**:82–90; discussion 90–1.
14. Ruben JD, Dally M, Bailey M *et al.* Cerebral radiation necrosis: incidence, outcomes, and risk factors with emphasis on radiation parameters and chemotherapy. *Int J Radiat Oncol Biol Phys* 2006;**65**:499–508.
15. de Wit MC, de Bruin HG, Eijkenboom W *et al.* Immediate post-radiotherapy changes in malignant glioma can mimic tumor progression. *Neurology* 2004;**63**:535–7.
16. Maxwell PH, Wiesener MS, Chang GW *et al.* The tumour suppressor protein VHL targets hypoxia-inducible factors for oxygen-dependent proteolysis. *Nature* 1999;**399**:271–5.
17. Kureshi SA, Hofman FM, Schneider JH *et al.* Cytokine expression in radiation-induced delayed cerebral injury. *Neurosurgery* 1994;**35**:822–9; discussion 829–30.
18. Ansari R, Gaber MW, Wang B *et al.* Anti-TNFA (TNF-alpha) treatment abrogates radiation-induced changes in vascular density and tissue oxygenation. *Radiat Res* 2007;**167**:80–6.
19. Mantych GJ, James DE, Devaskar SU. Jejunal/kidney glucose transporter isoform (Glut-5) is expressed in the human blood–brain barrier. *Endocrinology* 1993;**132**:35–40.
20. Siu A, Wind J, Iorgulescue J *et al.* Radiation necrosis following treatment of high grade glioma—a review of the literature and current understanding. *Acta Neurochir* 2012;**154**:191–201.
21. Wilson CM, Gaber MW, Sabek OM *et al.* Radiation-induced astrogliosis and blood-brain barrier damage can be abrogated using anti-TNF treatment. *Int J Radiat Oncol Biol Phys* 2009;**74**:934–41.
22. Nakae S, Saijo S, Horai R *et al.* IL-17 production from activated T cells is required for the spontaneous development of destructive arthritis in mice deficient in IL-1 receptor antagonist. *Proc Natl Acad Sci U S A* 2003;**100**:5986–90.
23. McCandless EE, Wang Q, Woerner BM *et al.* CXCL12 limits inflammation by localizing mononuclear infiltrates to the perivascular space during experimental autoimmune encephalomyelitis. *J Immunol* 2006;**177**:8053–64.
24. Cristillo AD, Highbarger HC, Dewar RL *et al.* Up-regulation of HIV coreceptor CXCR4 expression in human T lymphocytes is mediated in part by a cAMP-responsive element. *FASEB J* 2002;**16**:354–64.
25. Forster R, Kremmer E, Schubel A *et al.* Intracellular and surface expression of the HIV-1 coreceptor CXCR4/fusin on various leukocyte subsets: rapid internalization and recycling upon activation. *J Immunol* 1998;**160**:1522–31.
26. Burant CF, Takeda J, Brot-Laroche E *et al.* Fructose transporter in human spermatozoa and small intestine is GLUT5. *J Biol Chem* 1992;**267**:14523–6.
27. Gould GW, Holman GD. The glucose transporter family: structure, function and tissue-specific expression. *Biochem J* 1993;**295**:329–41.
28. Horikoshi Y, Sasaki A, Taguchi N *et al.* Human GLUT5 immunolabeling is useful for evaluating microglial status in neuropathological study using paraffin sections. *Acta Neuropathol* 2003;**105**:157–62.
29. Joost HG, Thorens B. The extended GLUT-family of sugar/polyol transport facilitators: nomenclature, sequence

characteristics, and potential function of its novel members (review). *Mol Membr Biol* 2001;**18**:247–56.
30. Kayano T, Burant CF, Fukumoto H *et al.* Human facilitative glucose transporters. Isolation, functional characterization, and gene localization of cDNAs encoding an isoform (GLUT5) expressed in small intestine, kidney, muscle, and adipose tissue and an unusual glucose transporter pseudogene-like sequence (GLUT6). *J Biol Chem* 1990;**265**:13276–82.
31. Mayhan WG. Cellular mechanisms by which tumor necrosis factor-alpha produces disruption of the blood–brain barrier. *Brain Res* 2002;**927**:144–52.
32. Sasaki A, Horikoshi Y, Yokoo H *et al.* Antiserum against human glucose transporter 5 is highly specific for microglia among cells of the mononuclear phagocyte system. *Neurosci Lett* 2003;**338**:17–20.
33. Lu DY, Tang CH, Yeh WL *et al.* SDF-1alpha up-regulates interleukin-6 through CXCR4, PI3 K/Akt, ERK, and NF-kappaB-dependent pathway in microglia. *Eur J Pharmacol* 2009;**613**:146–54.
34. Cruz-Orengo L, Holman DW, Dorsey D *et al.* CXCR7 influences leukocyte entry into the CNS parenchyma by controlling abluminal CXCL12 abundance during autoimmunity. *J Exp Med* 2011;**208**:327–39.
35. Hill WD, Hess DC, Martin-Studdard A *et al.* SDF-1 (CXCL12) is upregulated in the ischemic penumbra following stroke: association with bone marrow cell homing to injury. *J Neuropathol Exp Neurol* 2004;**63**:84–96.
36. Huang J, Li Y, Tang Y *et al.* CXCR4 antagonist AMD3100 protects blood–brain barrier integrity and reduces inflammatory response after focal ischemia in mice. *Stroke* 2013;**44**:190–7.

Futamura et al. Radiation Oncology 2014, 9:237
http://www.ro-journal.com/content/9/1/237

RADIATION ONCOLOGY

CASE REPORT Open Access

A case of radiation-induced osteosarcoma treated effectively by boron neutron capture therapy

Gen Futamura[1], Shinji Kawabata[1], Hiroyuki Siba[1], Toshihiko Kuroiwa[1], Minoru Suzuki[2], Natsuko Kondo[2], Koji Ono[2], Yoshinori Sakurai[3], Minoru Tanaka[4], Tomoki Todo[4] and Shin-Ichi Miyatake[5*]

Abstract

We treated a 54-year-old Japanese female with a recurrent radiation-induced osteosarcoma arising from left occipital skull, by reactor-based boron neutron capture therapy (BNCT). Her tumor grew rapidly with subcutaneous and epidural extension. She eventually could not walk because of cerebellar ataxia. The tumor was inoperable and radioresistant. BNCT showed a marked initial therapeutic effect: the subcutaneous/epidural tumor reduced without radiation damage of the scalp except hair loss and the patient could walk again only 3 weeks after BNCT. BNCT seems to be a safe and very effective modality in the management of radiation-induced osteosarcomas that are not eligible for operation and other treatment modalities.

Introduction

The incidence of radiation-induced sarcoma has been estimated to be between 0.03% and 0.3% of all patients who have received radiation therapy [1,2]. Radiation-induced osteosarcomas are being encountered more frequently as the use of radiation therapy becomes more common, and the number of long-term cancer survivors has increased. The original diagnostic criteria for radiation-induced osteosarcomas were proposed in 1948 by Cahan et al. [3], and a short latency period was recently accepted for these tumors [1,4,5]. The diagnosis of radiation-induced osteosarcoma must fulfill the following four criteria: (1) the sarcoma must arise in a previously irradiated field, (2) the sarcoma must be histologically distinct from the original neoplasm, (3) there was no evidence of tumor in the involved bone at the time of initial irradiation, and (4) there must be a latency period between the irradiation and the development of the sarcoma at least 3 years.

Radiation-induced osteosarcoma of the head is a devastating complication of radiation therapy. It is very rare but aggressive, with high recurrence and a poor prognosis [6]. The median overall survival time was reported to be 29 months [1]. Osteosarcoma is thought to be radioresistant [7,8]. Therefore, complete surgical resection has been described as the most important prognostic factor [9] and the first choice of treatment for radiation-induced osteosarcoma. However, if complete surgical resection is difficult (as it was in the present case), adjuvant chemotherapy and radiotherapy should be considered. These therapeutic effects have thus far been found to be insufficient, however. We report here the case of a patient with recurrent radiation-induced osteosarcoma who was treated effectively by boron neutron capture therapy (BNCT).

BNCT is based on the nuclear capture reactions that occur when non-radioactive boron-10 is irradiated with neutrons of the appropriate energy to yield high linear energy transfer (LET) alpha particles (4He) and recoiling lithium-7 (7Li) nuclei. Since these particles have short path-lengths of approximately one cell diameter, their lethality is primarily limited to boron-containing cells. Theoretically, high LET particles have the advantage to overcome radioresistance to photon radiotherapies (such as X-rays). BNCT can thus be regarded as tumor cell-selective and an intensive particle radiation modality with minimal damage to normal tissue, [10,11] even for X-ray-resistant tumors. Here we report a successfully treated a case of radiation-induced osteosarcoma by reactor-based BNCT.

Case report

A 54-year-old Japanese female was referred to our institute for treatment by BNCT of a recurrent radiation-induced

* Correspondence: neu070@poh.osaka-med.ac.jp
[5]Cancer Center, Osaka Medical College, Takatsuki, Japan
Full list of author information is available at the end of the article

osteosarcoma involving the left occipital bone. Ten years earlier, she was diagnosed with cancer of the uterine body and underwent resection surgery. Two years after that surgery, she underwent chemotherapy and whole-brain radiation therapy (WBRT, total 30 Gy with 10 fractions) including the cerebellum for brain metastasis. Six years after the WBRT, she was diagnosed with a radiation-induced osteosarcoma involving the left occipital bone, and she underwent resection surgery and successive chemotherapy using methotrexate. One year after that surgery and chemotherapy, the subcutaneous tumor appeared again in the left occipital region and rapidly enlarged over a period of only 3 months (Figure 1A). Magnetic resonance images (MRI) showed the epidural tumor invasion (Figure 2A and A'). Eventually, the patient could not walk because of acutely developing cerebellar ataxia. This tumor was diagnosed as a recurrence of the radiation-induced osteosarcoma in accord with the above Cahan's criteria [3].

We performed BNCT for the radiation-induced osteosarcoma because the lesion/normal brain (L/N) ratio of fluoride-labeled boronophenylalanine positron emission tomography (FBPA-PET) was enough high, as shown in Figure 3A and B (L/N ratio: 3.8) [12]. For the BNCT, neutron irradiation was applied at Kyoto University Reactor.

The patient was administered 500 mg/kg of BPA intravenously for 3.2 hours (200 mg/kg for initial 2 hours, prior to neutron irradiation, 100 mg/kg for 1.2 hours during neutron irradiation). The boron concentration in the blood was monitored by sampling every 1 hour after boron compound administration until neutron irradiation was completed. The boron concentrations from BPA in the tumor and normal brain were estimated from the L/N ratio of 18 F-BPA on PET. The neutron fluence rate was simulated by the dose-planning system, SERA (Idaho National Engineering and Environmental Laboratory, Idaho Falls, ID) and the total doses to the tumor and normal brain were simulated. The neutron irradiation time was determined not to exceed 13 Gy-Eq to the normal brain in accordance with our recent protocol of BNCT for high-grade meningiomas [10]. For this case, irradiation time was 70 minutes and B10 concentration of the venous blood was judged as 37.2 ppm during the neutron irradiation. Here, Gy-Eq (Gy: Gray) means an X-ray dose that can give biologically equivalent effects to total BNCT radiation. The scalp just above the tumor was covered with the bolus composed of sodium polyacrylate with 1 cm-thickness to gain the superficial neutron flux. After the treatment, the doses given were re-estimated precisely and are shown in Table 1. We hypothesized the boron concentrations of the blood, brain, and skin were equal, as we did in the previous BNCT. RBE and CBE values employed here were listed in Table 2.

Absorbed physical dose and X-ray-equivalent dose (Gy-Eq) are calculated with the following formula;

$$E_{Total} = E_{B10} + E_{Thermal} + E_{Fast} + E_{\gamma}$$

$$E_{B10} = (C_{BSH} \times CBE_{BSH} + C_{BPA} \times CBE_{BPA}) \times 7.43 \times 10^{-14} \times \Phi_{Thermal}$$

$$E_{Thermal} = N \times RBE_{Thermal} \times 6.78 \times 10^{-14} \times \Phi_{Thermal}$$

$$E_{Fast} = RBE_{Fast} \times D_{Fast}$$

$$E_{\gamma} = RBE_{\gamma} \times D_{\gamma}$$

D: physical absorbed dose (Gy),
ΦThermal: fluence of theraml neutron (cm-2),
N: nitrogen concentration (2%, here)
C: B10 concentration (ppm).

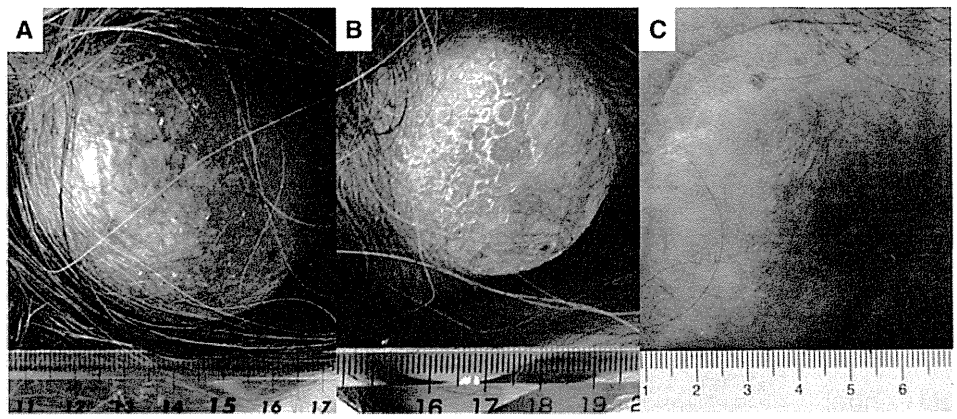

Figure 1 Marked improvement of the subcutaneous tumor at 3 weeks after the application of BNCT. A: Just prior to the BNCT; the tumor is elastic hard, and painful. **B**: Seven days after the BNCT; the tumor is soft and no longer painful. **C**: At 2 months after the BNCT, the tumor had shrunk drastically without radiation damage to the skin.

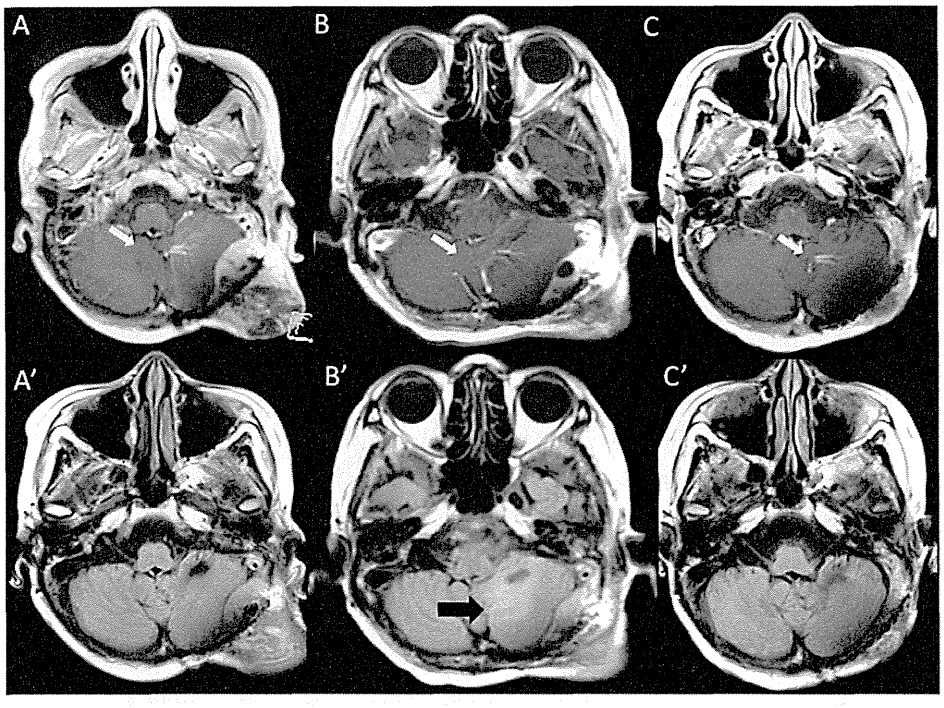

Figure 2 MRI of the patient's brain before and after the BNCT. White arrows indicate a venous angioma, which was recognized incidentally and judged as a sectional standard of MRI. **A**: Gd-enhanced T1-weighted MRI of the brain 1 month before the BNCT. There was a subcutaneous and epidural tumor mass. **B**: Gd-enhanced T1-weighted MRI at 4 days after BNCT. The tumor mass was reduced. **C**: Gd-enhanced T1-weighted MRI of the brain 3 months after BNCT. The tumor mass was further reduced. **A'**: Fluid-attenuated inversion recovery (FLAIR) MRI of the brain 1 month before BNCT. **B'**: FLAIR MRI of the brain 4 days after BNCT. The tumor mass was reduced, but the edema had worsened. A black arrow indicates the cerebellar edema. **C'**: FLAIR MRI of the brain 3 months after BNCT. The tumor mass was further reduced, and the edema had disappeared.

For this patient, we estimated that the minimum tumor and maximum normal brain and skin doses were 67.7, 12.7 and 12.4 Gy-Eq, respectively in the BNCT, simulated from F-BPA-PET imaging and the blood BPA concentration (Table 1).

At one day after the BNCT, the patient's gait disturbance was aggravated. Computed tomography at that time showed aggravation of peri-lesional edema (data not shown). Remarkably, the MRI taken 4 days after the BNCT demonstrated the definitive shrinkage of the mass, but the left cerebellar edema was still there (Figure 2B and B'). We then treated the edema with dehydrators and steroids. The symptoms gradually improved.

At only 3 weeks after the BNCT, the patient was able to walk again stably without aid. The subcutaneous tumor was reduced dramatically without radiation injury of the scalp, with time after BNCT, as shown in Figure 1B and C. The only adverse effect was hair loss in neutron-irradiation field, as shown in Figure 1C. MRI showed the further reduction of tumor and the disappearance of the cerebellar edema (Figure 2C and C'), 3 months after BNCT. Also F-BPA-PET taken 2 months after BNCT showed faint tracer uptake, indicating some metabolic change at least by this treatment (Figure 3A' and B', L/N ratio as 1.2).

Discussion

Radiation-induced osteosarcoma is not common. It has an aggressive nature, high recurrence rate, and poor prognosis. A standard therapy protocol has not yet been established for non-resectable tumors, but it was reported that particle radiotherapy (treatment with proton and carbon beams) had a therapeutic effect on these tumors [7,13].

In the present case, the tumor was chemo-resistant and difficult to totally resect because it invaded the left transverse and sigmoid venous sinuses. In addition, the subcutaneously extended tumor invaded the surface of the skin, and we thus suspected that a skin deficit due to surgery was inevitable and that particle radiotherapy for this tumor was likely to cause severe radiation-induced adverse effects on the scalp. The tumor was radiation-induced, and the cerebellum and overlying scalp had a history of X-ray treatment. Moreover, osteosarcomas have the characteristic of being radioresistant, i.e., X-ray-resistant. In light of these medical circumstances, we chose BNCT as the treatment modality for this patient. In the present case, the patient was successfully treated by BNCT without skin damage even though her tumor invaded the superficial scalp.

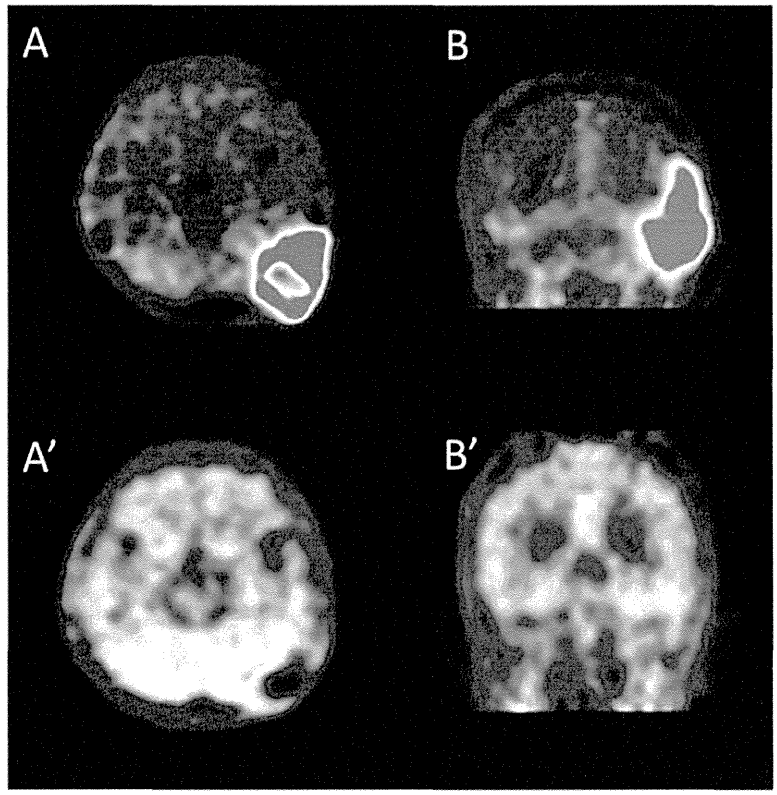

Figure 3 Fluoride-labeled boronophenylalanine-PET imaging of the brain before and after BNCT. Fluoride-labeled boronophenylalanine-PET imaging taken 1 month prior to BNCT (**A** and **B**) and 2 months after BNCT (**A'** and **B'**). **A** and **A'**: axial imaging, **B** and **B'**: coronal imaging. In **A** and **B**, L/N ratio was calculated as 5.0. This is theoretical proof of tumor selective destruction using BPA in BNCT. Also absorbed doses were simulated with this L/N ratio. 2 months after BNCT, **A'** and **B'** show the decreased L/N ratio as 1.2, indicating the marked effectiveness.

We recently reported the effectiveness of BNCT for radiation-refractory high-grade meningiomas [10]. In that report, we speculated that the difference in tumor shrinkage between the alpha and lithium particles provided by BNCT and other particles such as carbon and protons may be ascribed to the difference in LET noted above and their fraction size [10].

Other types of particle radiotherapy and some stereotactic radiotherapies which have been tried recently for tumors were applied as multi-fraction. The reduction of

Table 1 Estimated dose distribution at the central axis of neutron-irradiation field

Depth (cm)	Total dose (tumor) (Gy-eq)	Total dose (skin) (Gy-eq)	Total dose (mucosa) (Gy-eq)	Total dose (brain) (Gy-eq)	Thermal neutron (Gy-eq)	Fast neutron (Gy-eq)	γ-ray (Gy-eq)	Boron dose (tumor) (Gy-eq)
0.00	5.28E + 01	1.24E + 01	2.08E + 01	8.37E + 00	5.05E-01	2.13E + 00	1.00E + 00	4.92E + 01
0.50	6.79E + 01	----------	2.61E + 01	9.90E + 00	6.56E-01	1.87E + 00	1.22E + 00	6.41E + 01
1.00	8.06E + 01	----------	3.06E + 01	1.12E + 01	7.83E-01	1.64E + 00	1.43E + 00	7.67E + 01
1.50	8.47E + 01	----------	3.20E + 01	1.16E + 01	8.24E-01	1.35E + 00	1.63E + 00	8.09E + 01
2.00	9.00E + 01	----------	3.39E + 01	1.21E + 01	8.77E-01	1.17E + 00	1.80E + 00	8.62E + 01
2.50	9.38E + 01	----------	3.53E + 01	1.26E + 01	9.13E-01	1.11E + 00	1.92E + 00	8.98E + 01
3.00	9.55E + 01	----------	3.58E + 01	1.27E + 01	9.31E-01	9.77E-01	2.02E + 00	9.16E + 01
3.50	9.53E + 01	----------	3.57E + 01	1.27E + 01	9.30E-01	8.63E-01	2.09E + 00	9.14E + 01
4.00	9.18E + 01	----------	3.44E + 01	1.22E + 01	8.94E-01	7.72E-01	2.11E + 00	8.80E + 01
4.50	8.62E + 01	----------	3.24E + 01	1.16E + 01	8.38E-01	6.91E-01	2.10E + 00	8.26E + 01
5.00	7.97E + 01	----------	3.00E + 01	1.08E + 01	7.74E-01	6.18E-01	2.08E + 00	7.62E + 01
5.50	7.15E + 01	----------	2.70E + 01	9.79E + 00	6.93E-01	5.54E-01	1.99E + 00	6.82E + 01
5.80	6.77E + 01	----------	2.56E + 01	9.31E + 00	6.55E-01	5.12E-01	1.95E + 00	6.45E + 01

Table 2 RBE (relative biological effectiveness) factor

Radiation	Tumor	Brain	Skin
Thermal neuton	3.0	3.0	3.0
Epithermal neutron	3.0	3.0	3.0
^{10}B (n,α)^{7} Li: BPA	3.8	1.35	2.5
γ-ray dose	1.0	1.0	1.0

the tumor mass was thus not very prominent, and it was difficult to improve the patients' symptoms by means other than BNCT. BNCT can deliver high dose particles in a tumor-selective fashion in a single session, and in some cases the resulting reduction of the tumor was fast; this rapid shrinkage might contribute to the prompt elimination of symptoms [10]. Indeed, the present patient, within a very short time, exhibited improvement of her gait disturbance due to cerebellar ataxia.

Only a couple of articles were published with regard to pre-clinical study of BNCT for osteosarcoma in in vitro cell culture and animal experiments [14-17]. Among them, Russian research group reported successful treatment of dog osteosarcoma case by BNCT. Also only one preliminary report was published with regard to a BNCT-treated osteosarcoma case in head and neck region with limited description, so far [18]. We are not sure of the compound biological effectiveness (CBE) of BPA for osteosarcomas, and we were only able to estimate CBE as being the same for glioblastoma (i.e., 3.8) [19] as we did for high-grade meningioma [10]. For the estimation of the prescribed dose for this case, we adopted the reported value of CBE and relative biological effectiveness of neutron itself for tumors and normal tissues [20]. Thereafter the estimated tumor dose was uncertain in this case. However, as a result of the BNCT, the tumor shrank rapidly, the patient's clinical symptoms improved, metabolically scarce uptake of the amino-acid tracer was observed in the follow-up PET imaging and no serious damage was observed in the scalp and brain, so far at 6 months after BNCT, although the observation period was short.

Based on this outcome, we found that BNCT was an effective treatment for our patient. However, careful follow-up or the use of bevacizumab may be necessary in some cases [21], because WBRT that has been already performed may cause brain radiation necrosis.

We experienced only a case of successful treatment of BNCT for radiation-induced osteosacoma. Hopefully these potential therapeutic effects will be applicable for non-radiation-induced osteosarcomas which are generally refractory for other treatment modalities.

Conclusions

BNCT is an effective treatment for non-resectable radiation-induced skull osteosarcoma. We suggest that BNCT is the only effective therapy for tumors that have invaded the skin. Further applications of BNCT for similar cases are expected.

Competing interests

The authors declare that they have no competing interests.

Authors' contributions

S-IM conceived of the study and participated in the follow-up of the patient. GF, SK, NK, MS and KO applied BNCT in the atomic reactor. YS simulated BNCT dose. HS and TK participated in patient care in the hospital. MT and TT referred the patient for S-IM and also participated in the patient care and follow-up at the out-patient clinic. All authors read and approved the final manuscript.

Acknowledgement

We appreciate Dr. Silva Bortolussi, National Institute for Nuclear Physics (INFN) Section of Pavia, Italy for the critical reading of the manuscript and fruitful discussion.

Author details

[1]Department of Neurosurgery, Osaka Medical College, Takatsuki, Japan. [2]Particle Radiation Oncology Research Center, Kyoto University Research Reactor Institute, Kumatori, Japan. [3]Division of Radiation Life Science, Kyoto University Research Reactor Institute, Kumatori, Japan. [4]Division of Innovative Cancer Therapy, and Department of Surgical Neuro-Oncology The Institute of Medical Science, The University of Tokyo, Tokyo, Japan. [5]Cancer Center, Osaka Medical College, Takatsuki, Japan.

Received: 8 September 2014 Accepted: 14 October 2014
Published online: 04 November 2014

References

1. Patel AJ, Rao VY, Fox BD, Suki D, Wildrick DM, Sawaya R, DeMonte F: **Radiation-induced osteosarcomas of the calvarium and skull base.** *Cancer* 2011, 117:2120–2126.
2. Amendola BE, Amendola MA, McClatchey KD, Miller CH Jr: **Radiation-associated sarcoma: a review of 23 patients with postradiation sarcoma over a 50-year period.** *Am J Clin Oncol* 1989, 12:411–415.
3. Cahan WG, Woodard HQ, Higinbotham N, Stewart F, Coley B: **Sarcoma arising in irradiated bone; report of 11 cases.** *Cancer* 1948, 1:3–29.
4. Arlen M, Higinbotham NL, Huvos AG, Marcove RC, Miller T, Shah IC: **Radiation-induced sarcoma of bone.** *Cancer* 1971, 28:1087–1099.
5. Murray EM, Werner D, Greeff EA, Taylor DA: **Postradiation sarcomas: 20 cases and a literature review.** *Int J Radiat Oncol Biol Phys* 1999, 45:951–961.
6. Patel RD, Gadgil NM, Khare M, Majethia N: **Radiation-induced intracranial osteosarcoma: a case report.** *J Postgrad Med* 2014, 60:218–219.
7. Imai R, Kamada T, Tsuji H, Tsujii H, Tsuburai Y, Tatezaki S: **Cervical spine osteosarcoma treated with carbon-ion radiotherapy.** *Lancet Oncol* 2006, 7:1034–1035.
8. Mankin HJ, Hornicek FJ, Rosenberg AE, Harmon DC, Gebhardt MC: **Survival data for 648 patients with osteosarcoma treated at one institution.** *Clin Orthop Relat Res* 2004, 429:286–291.
9. Granados-Garcia M, Luna-Ortiz K, Castillo-Oliva HA, Villavicencio-Valencia V, Herrera-Gomez A, Mosqueda-Taylor A, Aguilar-Ponce JL, Poitevin-Chacon A: **Free osseous and soft tissue surgical margins as prognostic factors in mandibular osteosarcoma.** *Oral Oncol* 2006, 42:172–176.
10. Kawabata S, Hiramatsu R, Kuroiwa T, Ono K, Miyatake S: **Boron neutron capture therapy for recurrent high-grade meningiomas.** *J Neurosurg* 2013, 119:837–844.
11. Kawabata S, Yang W, Barth RF, Wu G, Huo T, Binns PJ, Riley KJ, Ongayi O, Gottumukkala V, Vicente MG: **Convection enhanced delivery of carboranylporphyrins for neutron capture therapy of brain tumors.** *J Neuro-Oncol* 2011, 103:175–185.
12. Miyashita M, Miyatake S, Imahori Y, Yokoyama K, Kawabata S, Kajimoto Y, Shibata MA, Otsuki Y, Kirihata M, Ono K, Kuroiwa T: **Evaluation of fluoride-labeled boronophenylalanine-PET imaging for the study of radiation effects in patients with glioblastomas.** *J Neuro-Oncol* 2008, 89:239–246.
13. Blattmann C, Oertel S, Schulz-Ertner D, Rieken S, Haufe S, Ewerbeck V, Unterberg A, Karapanagiotou-Schenkel I, Combs SE, Nikoghosyan A, Bischof M, Jakel O: **Non-randomized therapy trial to determine the safety and**

efficacy of heavy ion radiotherapy in patients with non-resectable osteosarcoma. *BMC Cancer* 2010, 10:96.
14. Bortolussi S, Ciani L, Postuma I, Protti N, Luca R, Bruschi P, Ferrari C, Cansolino L, Panza L, Ristori S, Altieri S: Boron concentration measurements by alpha spectrometry and quantitative neutron autoradiography in cells and tissues treated with different boronated formulations and administration protocols. *Appl Radiat Isot* 2014, 88:78–80.
15. Ferrari C, Zonta C, Cansolino L, Clerici AM, Gaspari A, Altieri S, Bortolussi S, Stella S, Bruschi P, Dionigi P, Zonta A: Selective uptake of p-boronophenylalanine by osteosarcoma cells for boron neutron capture therapy. *Appl Radiat Isot* 2009, 67:S341–S344.
16. Mitin VN, Kulakov VN, Khokhlov VF, Sheino LN, Bass LP, Kozolofskaya NG, Zaitsev KN, Potnov AA, Yagnikov SA, Shiraev SV: BNCT for Canine Osteosarcoma from Advances in Neutron Capture Therapy 2006. In *Proceedings of 12th International Congress on Neutron Capture Therapy. 9–13 October 2006.* Edited by Nakagawa Y. 2006:135–138.
17. Hsu CF, Lin SY, Peir JJ, Liao JW, Lin YC, Chou FI: Potential of usingboric acid as a boron drug for boron neutron capture therapy for osteosarcoma. *Appl Radiat Isot* 2011, 69:1782–1785.
18. Kato I, Ono K, Sakurai Y, Ohmae M, Maruhashi A, Imahori Y, Kirihata M, Nakazawa M, Yura Y: Effectiveness of BNCT for recurrent head and neck malignancies. *Appl Radiat Isot* 2004, 61:1069–1073.
19. Miyatake S, Kawabata S, Kajimoto Y, Aoki A, Yokoyama K, Yamada M, Kuroiwa T, Tsuji M, Imahori Y, Kirihata M, Sakurai Y, Masunaga S, Nagata K, Maruhashi A, Ono K: Modified boron neutron capture therapy for malignant gliomas performed using epithermal neutron and two boron compounds with different accumulation mechanisms: an efficacy study based on findings on neuroimages. *J Neurosurg* 2005, 103:1000–1009.
20. Coderre JA, Morris GM: The radiation biology of boron neutron capture therapy. *Radiat Res* 1999, 151:1–18.
21. Miyatake S, Kawabata S, Hiramatsu R, Furuse M, Kuroiwa T, Suzuki M: Boron neutron capture therapy with bevacizumab may prolong the survival of recurrent malignant glioma patients: four cases. *Radiat Oncol* 2014, 9:6.

doi:10.1186/s13014-014-0237-z
Cite this article as: Futamura *et al.*: A case of radiation-induced osteosarcoma treated effectively by boron neutron capture therapy. *Radiation Oncology* 2014 9:237.

Miyatake et al. Radiation Oncology 2014, 9:6
http://www.ro-journal.com/content/9/1/6

RADIATION ONCOLOGY

CASE REPORT Open Access

Boron neutron capture therapy with bevacizumab may prolong the survival of recurrent malignant glioma patients: four cases

Shin-Ichi Miyatake[1*], Shinji Kawabata[1], Ryo Hiramatsu[1], Motomasa Furuse[1], Toshihiko Kuroiwa[1] and Minoru Suzuki[2]

Abstract

Background and importance: Recurrent malignant gliomas (RMGs) are very difficult to control, and no standard treatments have been established for them. We performed boron neutron capture therapy (BNCT) for patients with RMG. BNCT enables high-dose particle radiation to be applied selectively to tumor cells. However, RMG cases generally receive nearly 60 Gy X-ray irradiation prior to re-irradiation by BNCT. Therefore, even with tumor-selective particle radiation BNCT, radiation necrosis in the brain and symptomatic pseudoprogression may develop. In four of our recent patients with RMG after BNCT, we applied the anti-VEGF antibody bevacizumab to treat two pathological entities. This approach appeared to prolong survival. Here we present the case reports of these four consecutive patients with RMG and discuss the novel use of bevacizumab in this context.

Clinical presentation: Four patients with RMGs were treated with BNCT at our institutes. Upon the referral for BNCT, they were assessed as belonging to the recursive partitioning analysis (RPA) class 3 (n = 3 patients) or RPA class 4 (n = 1 patient) (the RPA classification for RMG was advocated by Carson et al. in 2007). The estimated median survival times for RPA classes 3 and 4 were 3.8 and 10.8 months, respectively, after some treatment at the recurrence. We applied BNCT for these four patients and administered bevacizumab when the lesions were considered radiation necrosis or symptomatic pseudoprogression. The class 3 patients survived after the BNCT for 14, 16.5 and > 23 months, and the class 4 patient survived > 26 months, with favorable improvements in clinical symptoms.

Conclusion: BNCT with the addition of bevacizumab for radiation necrosis or symptomatic pseudoprogression improved the clinical symptoms and prolonged the survival in RMG patients.

Keywords: Bevacizumab, Boron neutron capture therapy, Recurrent malignant glioma

Background

The prognosis of recurrent malignant gliomas (RMGs) is poor, and no standard treatment has been established [1]. Since 2002 at our institute, we have been applying a form of tumor-selective particle radiation, boron neutron capture therapy (BNCT), for RMGs and observed favorable survival outcomes [2,3]. BNCT is a biochemically targeted radiotherapy based on the nuclear capture and fission reactions that occur when non-radioactive boron-10, which is a constituent of natural elemental boron, is irradiated with low-energy thermal neutrons to yield high-linear-energy transfer alpha particles and recoiling lithium-7 nuclei. These particles are released within a very short range such as 9 μm, and therefore the cytotoxic effects are confined within boron-10-containing cells [4].

Boron-10-containing compounds can be accumulated selectively in tumor cells by several mechanisms. For example, boronophenylalanine (BPA) is selectively and preferentially accumulated in tumor cells via the augmented metabolism of amino acids compared to normal cells. Even with this novel and selective particle radiation technique, radiation damage — chiefly radiation necrosis (RN) and symptomatic pseudoprogression (psPD) — often occurs [5,6]. The radiation damage is especially likely in RMG cases, because full-dose X-ray treatment (XRT) is generally part of the treatment history in such cases.

Bevacizumab (BV), an anti-vascular endothelial growth factor (VEGF) antibody, has recently been used for the

* Correspondence: neu070@poh.osaka-med.ac.jp
[1]Department of Neurosurgery, Osaka Medical College, Osaka, Japan
Full list of author information is available at the end of the article

treatment of symptomatic RN [7,8]. Based on our analysis of human RN surgical specimens, we previously demonstrated that the edema in RN is caused by the overexpression of VEGF in reactive astrocytes [9]. Following this determination, we used BV in an attempt to control the symptomatic RN and the symptomatic psPD encountered after BNCT for RMGs [5,7]. Here we present a case series report of our last four consecutive cases of RMG treated with BNCT and BV, with >18-month observation periods. All four patients had RMGs after primary treatment with XRT and chemotherapy consisting chiefly of temozolomide (TMZ). The patients' profiles and survival data are listed in Table 1. Three of the patients were classified as recursive partitioning analysis (RPA) (advocated by Carson et al. in 2007 [1]) class 3 and one was classified as RPA class 4.

Case presentation

Case 1

A 44-year-old male's craniotomy showed anaplastic astrocytoma. He received standard chemoradiotherapy (XRT 60 Gy with TMZ). Unfortunately the lesion recurred with aggravation of aphasia and right hemiparesis, which forced him to retire from his job. The Karnofsky performance status (KPS) was 70%, and he was classified as RPA class 3. The patient was then referred to our institute for BNCT. Upon referral, MRI showed a slightly enhanced lesion with mild perifocal edema (Figure 1). A simultaneous fluorine-18-labeled BPA positron emission tomography (F-BPA-PET) image showed marked tracer uptake in the left parietofrontal region (Figure 1), with a 6.0 lesion/normal (L/N) brain ratio of the tracer, indicating that the lesion was a highly malignant tumor. BNCT was applied for this patient according to our recent protocol for RMGs and meningiomas [10]. Briefly, only BPA was administered over a 2-hr period (200 mg/kg/hr) just prior to and during the neutron irradiation (100 mg/kg/hr). The neutron irradiation time was decided based on a simulation not to exceed 12.0 Gy-Eq (Gray-equivalent) for the peak brain dose. The 10-B concentration in the blood during the neutron irradiation was 23.0 parts per million (ppm). By BNCT, the maximum brain dose, maximum tumor dose, and minimum tumor dose were estimated as 11.4, 118, and 36.1 Gy-Eq, respectively. Here, "Gy-Eq" corresponds to the biologically equivalent X-ray dose that would have equivalent effects on tumors and on the normal brain. The dose estimation was performed by the measurement of blood boron concentration and F-BPA-PET data prior to neutron irradiation as described elsewhere [2,6,10].

After the BNCT, an MRI showed gradual enlargement of both perifocal edema and contrast enhancement, whereas sequential F-BPA-PET showed a favorable decrease of tracer uptake (Figure 1, lower panel). F-BPA-PET was originally developed to estimate the absorbed dose in BNCT, as described above [2,11,12]. The background uptake of the tracer F-BPA is very low compared to that of fluorodeoxy-glucose and even compared to that of methionine as a tracer. Thereafter, RN and psPD have been differentially diagnosed from tumor progression by F-BPA-PET [6,13]. Ten months after the BNCT, the patient's KPS worsened to 60%, and so we administered BV 5 mg/kg biweekly, three times. Just prior to the BV administration, F-BPA-PET showed a more decreased L/N ratio, which indicated that the aggravation shown by MRI was RN and not a recurrence of the tumor. After the BV treatment, MRI showed improvement of the perilesional edema and a decrease in contrast enhancement. The BV treatment stabilized the patient's symptoms for 6 months but then his symptoms recurred, prompting us to perform a re-challenge with BV another three times. The patient is now stable and doing well, 23 months after the BNCT (Table 1).

Case 2

A 41-year-old man underwent surgery for his right parietal glioblastoma (GBM) with subtotal excision. Standard treatment with XRT and TMZ was performed, but the tumor recurred 5 months after the surgery. Upon referral for BNCT, the patient's KPS was assessed as 90% and he was classified as RPA class 4. MRI showed a definitively enhanced lesion with moderate perifocal edema (Figure 2). A simultaneous F-BPA-PET image showed marked tracer uptake in the right parietal region with a 3.8 L/N ratio of the tracer, indicating that the lesion was a recurrent malignant tumor and not psPD (Figure 2,

Table 1 The background of the four patients with recurrent malignant glioma (RMG)

Case No.	Age	Sex	Hist.	RPA class	Irradiated dose (Gy-Eq)			BV cycles	PsPD or RN	Survival (Months from BNCT)
					Brain (Max)	Tumor (Max)	Tumor (Mini)	(Months from BNCT)		
1	43	M	AA	3	11.4	118	36.1	3 (11 M)	RN	23 M, alive
2	41	M	GBM	4	12.1	88.5	36.6	4 (14 M)	RN	26 M, alive
3	60	M	AA	3	10.8	110	82.3	6 (4 M)	PsPD	16.5 M
4	34	F	AOA	3	11.5	71.6	30.1	6 (2 M)	PsPD	14 M

Hist, histology; RPA, recursive portioning analysis; BV, Bevacizumab; PsPD, pseudoprogression; RN, radiation necrosis; BNCT, boron neutron capture therapy.

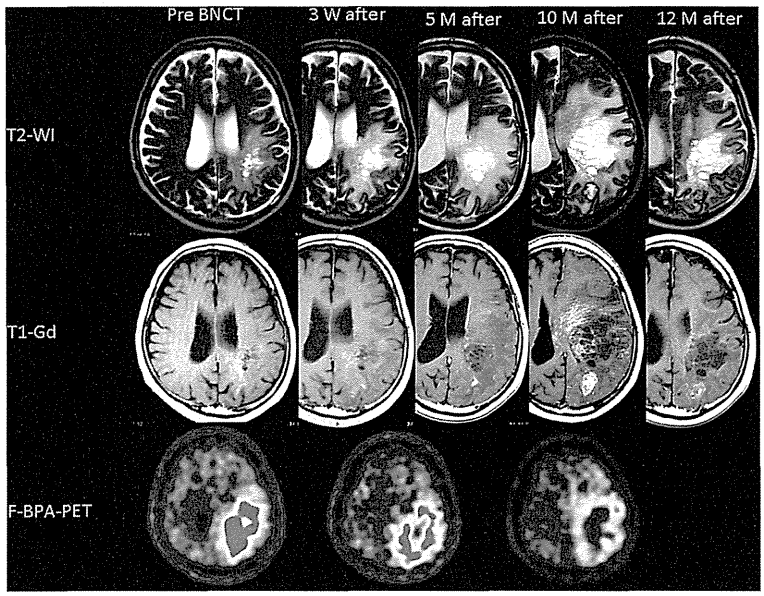

Figure 1 Sequential change of T2-weighted MRI (upper column), Gd-enhanced T1-weighted MRI (middle column) and F-BPA-PET (lower column) of Case 1, a 44-year-old male. The timing of the MRIs is depicted above the MRIs. F-BPA-PET images were taken just before the BNCT and at 1 month and 10 months after the BNCT. These PET images show the gradual decrease of the tracer uptake as a promising effect of the BNCT. BV was started 10 months after the BNCT, and the MRI showed marked improvement of both perifocal edema and contrast enhancements by BV treatment.

lower panel). He was treated with BNCT, with the same protocol as Case 1. The boron-10 concentration in the blood during the neutron irradiation was 30.2 ppm. By BNCT, the maximum brain dose, maximum tumor dose, and minimum tumor dose were estimated as 12.1, 88.5, and 36.6 Gy-Eq, respectively. One week after the BNCT, a contrast-enhanced T1-weighted MRI showed a marked shrinkage of the mass, and that at 3 months later showed slight enlargement of the enhanced lesion, which was presumed to be psPD. Periodic MRIs showed

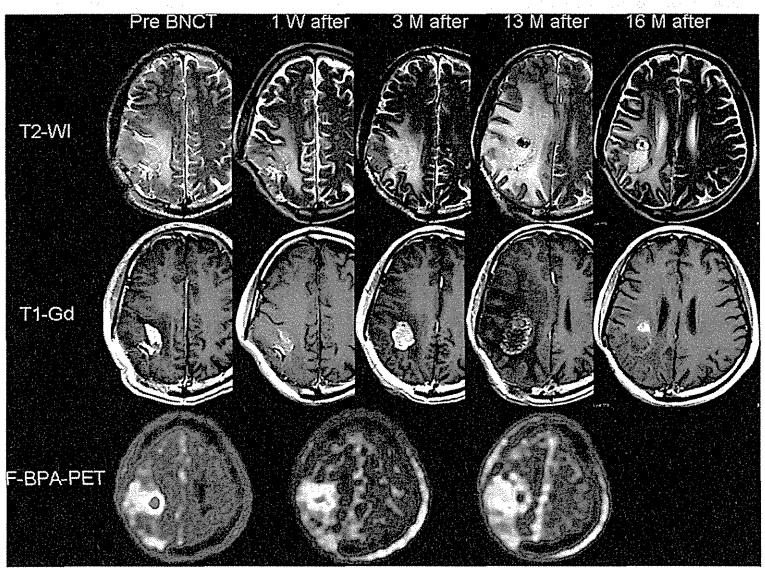

Figure 2 Sequential change of T2-weighted MRI (upper column), Gd-enhanced T1-weighted MRI (middle column) and F-BPA-PET (lower column) of Case 2, a 41-year-old man. The timing of the MRI is depicted above the MRI. F-BPA-PET images were taken just before the BNCT, 1 month after and 12 months after the BNCT. These PET images show the gradual decrease of the tracer uptake as a promising effect of BNCT. BV was started 13 months after the BNCT, and an MRI showed a marked positive effect of the BV treatment on the perifocal edema and contrast enhancements.

gradual enlargement of both the enhanced lesion and perifocal edema, whereas F-BPA-PET showed a gradual decrease of the tracer uptake. The final L/N ratio, 1 year after BNCT, was 2.3. This L/N ratio and the MRI 13 months after the BNCT suggested that the lesion was RN.

The patient was not able to continue his work as a cook, and we decided to begin intravenous BV treatment biweekly (5 mg/kg). After four treatments, MRI showed marked improvement in the perifocal edema and left hemiparesis. The patient is now doing well and has resumed his work as a cook, 26 months after the BNCT, without tumor progression or recurrence of the RN.

Case 3

A 56-year-old male experienced speech disturbance and mild right hemiparesis. First he received a craniotomy with a diagnosis of gemistocytic astrocytoma, followed by fractionated XRT (total 50 Gy) and repetitive chemotherapy with nitrosourea. Three years later, a recurrent lesion appeared with Gd enhancement on MRI. Re-craniotomy revealed GBM histologically. After surgery, the enhanced lesion gradually grew and the patient's sensory aphasia worsened despite the repeated administration of TMZ. He was referred to our institute for BNCT. Upon his referral, he was assessed as RPA class 3. The boron-10 concentration in the blood during the neutron irradiation was 30.0 ppm. Using BNCT, the maximum brain dose, maximum tumor dose, and minimum tumor dose were estimated as 10.8, 110, and 82.3 Gy-Eq, respectively, as shown in Table 1. His right hemiparesis and aphasia gradually worsened after the BNCT, even with an escalating dose of corticosteroids. Four months after the BNCT, a follow-up MRI and F-BPA-PET suggested that the lesion was symptomatic psPD, not tumor progression. The patient was successfully treated with BV, as we recently reported, along with the periodic changes of the neuroimages and the detailed clinical course [5]. We lost this patient to local tumor progression 16.5 months after the BNCT.

Case 4

A 27-year-old female manifested left hemiparesis. A right frontal enhanced mass was removed gross/totally, and the histological diagnosis was anaplastic oligo-astrocytoma. She received fractionated XRT (total 72 Gy) and repetitive chemotherapy with nitrosourea. The lesion recurred and re-craniotomy was performed 4 years later, with the same pathological diagnosis. This was followed by TMZ chemotherapy. Unfortunately, a recurrence was confirmed by MRI and she was referred to us for BNCT. The boron-10 concentration in the blood during the neutron irradiation was 21.4 ppm. By BNCT, the maximum brain dose, maximum tumor dose, and minimum tumor dose were 11.5, 71.6, and 30.1 Gy-Eq, respectively (Table 1). After the BNCT, her hemiparesis gradually became aggravated despite an increased dose of corticosteroids. MRI taken 2 months after the BNCT showed an enlarged enhanced lesion with increased perilesional edema. We judged this aggravation as symptomatic psPD. We started BV treatment for her. The patient was bedridden just prior to the BV treatment, but after two BV treatments her hemiparesis improved markedly and she could walk. Her neuroimages and clinical symptoms showed marked improvement, as we reported previously [5]. Unfortunately we lost her because of tumor extension to the opposite hemisphere 14 months after the BNCT.

The neuroimages, including F-BPA-PET scans of Cases 3 and 4, were published elsewhere [5] and thus are not included in this brief report.

Discussion

In comparison with many Phase I and II trials for RMG [1], BNCT showed a marked survival benefit for RMG in our previous study, in which BV was not used [3]. Briefly, BNCT resulted in median survival times (MSTs) (months and 95% confidence intervals) as follows: for all RPA classes (Classes 1–7), 10.8 (7.3–12.8) (n = 22), and in the poor-prognosis group (RPA class 3 + 7), 9.1(4.4–11.0) (n = 11). In a meta-analysis reported in the Journal of Clinical Oncology [1], the MSTs in all RPA classes and in the poor-prognosis group (RPA class 3 + 7) were 7.0 (6.2–8.0) (n = 310) and 4.4 (3.6–5.4) (n = 129), respectively. These data showed the superiority of BNCT for RMGs, especially in poor-prognosis groups. In comparison, our previous data showed MSTs of RPA class 3 and 4 as 7.3 and 12.0 months, respectively, although the number of the patients was quite limited: 4 cases in class 3 and 3 cases in class 4 [3].

In our recent patients undergoing BNCT for RMGs, we have begun to treat RN or symptomatic psPD aggressively by administering BV. We applied intravenous BV treatment for four recent RMG patients treated with BNCT at our institute and in whom we encountered RN or symptomatic psPD; these cases are reported here. Three of these four patients were classified as RPA class 3 and one as class 4 (Table 1). The estimated survival time of class 3 patients is 3.8 months and that of class 4 patients is 10.8 months [1]. Our three class 3 patients survived for 14, 16.5, and > 23 months, and the class 4 patient has survived for over 26 months.

At a glance, BNCT with BV seemed to prolong the survival of RMGs strikingly in comparison not only with Carson's data set but also with our previous BNCT data. Although of course no definitive conclusion can be drawn from such a small number of cases.

In our limited experience, there is no obvious histological difference between RN and psPD [6]. The center part of each pathology is characterized as histological necrosis, and

marked angiogenesis is observed in the boundary of the necrotic core and normal brain tissue [9]. Clinically, most psPD occurs at a relatively early stage after intensive treatments and is self-limiting without severe sequelae [14]. In most cases, psPD improves over time without intensive treatments. On the other hand, RN often shows severe symptoms and occurs at least a half year after radiotherapy. Thereafter, symptomatic psPD is especially difficult to distinguish from RN. In Table 1, we distinguish them only from the duration of the symptomatic onset after BNCT.

We have described herein the use of BV for RN or psPD after BNCT. BV was approved for the treatment of RMGs as an anticancer agent [15,16], and several trials of re-irradiation using XRT or hypo-fractionated stereotactic radiotherapy in combination with BV just before radiotherapy for RMGs have recently been conducted, with favorable preliminary safety and response results [17-19]. The authors of those reports described the role of BV not only as an anticancer agent but also for normalizing the perfusion pressure and oxygenation effects during irradiation. BV may also prevent RN and symptomatic psPD after re-irradiation.

We are now planning a prospective clinical trial of BNCT using BV immediately after neutron irradiation for RMG patients with poor prognosis (class 3 + 7). We are also conducting a clinical trial of BNCT for RMGs using a small accelerator in-hospital, instead of an atomic reactor. We hope to determine whether accelerator-based BNCT with BV could be used as a standard treatment for RMGs.

Conclusion

BNCT with the addition of BV for radiation necrosis or symptomatic pseudoprogression improved the clinical symptoms and might prolong the survival of RMG patients.

Consent

Written informed consent was obtained from the patient for the publication of this report and any accompanying images.

Abbreviations

BNCT: Boron neutron capture therapy; BPA: Boronophenylalanine; BV: Bevacizumab; GBM: Glioblastoma; Gy-Eq: Gray-equivalent; KPS: Karnofsky performance status; L/N: Lesion/normal; PET: Positron emission tomography; ppm: parts per million; psPD: pseudoprogression; RMG: Recurrent malignant gliomas; RN: Radiation necrosis; RPA: Recursive portioning analysis; TMZ: Temozolomide; XRT: X-ray treatment.

Competing interests

There is no conflict of interest to disclose for any of the authors.

Authors' contributions

S-IM conceived of the study and participated in the follow-up of patients. SK, RH, and MS applied BNCT in the atomic reactor. MF followed the patients with bevacizumab. TK selected the patients for BNCT. All authors read and approved the final manuscript.

Acknowledgments

This work was supported in part by a Grant-in-Aid for Scientific Research (B) (19390385) from the Japanese Ministry of Education, Culture, Sports, Science, and Technology to S-IM.

Author details

[1]Department of Neurosurgery, Osaka Medical College, Osaka, Japan. [2]Radiation Oncology and Particle Radiation Oncology Research Center, Research Reactor Institute, Kyoto University, Kyoto, Japan.

Received: 5 November 2013 Accepted: 2 January 2014
Published: 6 January 2014

References

1. Carson KA, Grossman SA, Fisher JD, Shaw EG: **Prognostic factors for survival in adult patients with recurrent glioma enrolled onto the new approaches to brain tumor therapy CNS consortium phase I and II clinical trials.** *J Clin Oncol* 2007, **25**:2601–2606.
2. Miyatake S, Kawabata S, Kajimoto Y, Aoki A, Yokoyama K, Yamada M, Kuroiwa T, Tsuji M, Imahori Y, Kirihata M, *et al*: **Modified boron neutron capture therapy for malignant gliomas performed using epithermal neutron and two boron compounds with different accumulation mechanisms: an efficacy study based on findings on neuroimages.** *J Neurosurg* 2005, **103**:1000–1009.
3. Miyatake S, Kawabata S, Yokoyama K, Kuroiwa T, Michiue H, Sakurai Y, Kumada H, Suzuki M, Maruhashi A, Kirihata M, Ono K: **Survival benefit of Boron neutron capture therapy for recurrent malignant gliomas.** *J Neurooncol* 2009, **91**:199–206.
4. Barth RF, Vicente MG, Harling OK, Kiger WS 3rd, Riley KJ, Binns PJ, Wagner FM, Suzuki M, Aihara T, Kato I, Kawabata S: **Current status of boron neutron capture therapy of high grade gliomas and recurrent head and neck cancer.** *Radiat Oncol* 2012, **7**:146.
5. Miyatake S, Furuse M, Kawabata S, Maruyama T, Kumabe T, Kuroiwa T, Ono K: **Bevacizumab treatment of symptomatic pseudoprogression after boron neutron capture therapy for recurrent malignant gliomas. Report of 2 cases.** *Neuro Oncol* 2013, **15**:650–655.
6. Miyatake S, Kawabata S, Nonoguchi N, Yokoyama K, Kuroiwa T, Matsui H, Ono K: **Pseudoprogression in boron neutron capture therapy for malignant gliomas and meningiomas.** *Neuro Oncol* 2009, **11**:430–436.
7. Furuse M, Kawabata S, Kuroiwa T, Miyatake S: **Repeated treatments with bevacizumab for recurrent radiation necrosis in patients with malignant brain tumors: a report of 2 cases.** *J Neurooncol* 2011, **102**:471–475.
8. Levin VA, Bidaut L, Hou P, Kumar AJ, Wefel JS, Bekele BN, Prabhu S, Loghin M, Gilbert MR, Jackson EF: **Randomized double-blind placebo-controlled trial of bevacizumab therapy for radiation necrosis of the central nervous system.** *Int J Radiat Oncol Biol Phys* 2011, **79**:1487–1495.
9. Nonoguchi N, Miyatake S, Fukumoto M, Furuse M, Hiramatsu R, Kawabata S, Kuroiwa T, Tsuji M, Fukumoto M, Ono K: **The distribution of vascular endothelial growth factor-producing cells in clinical radiation necrosis of the brain: pathological consideration of their potential roles.** *J Neurooncol* 2011, **105**:423–431.
10. Kawabata S, Hiramatsu R, Kuroiwa T, Ono K, Miyatake S: **Boron neutron capture therapy for recurrent high-grade meningiomas.** *J Neurosurg* 2013, **119**:837–844.
11. Imahori Y, Ueda S, Ohmori Y, Sakae K, Kusuki T, Kobayashi T, Takagaki M, Ono K, Ido T, Fujii R: **Positron emission tomography-based boron neutron capture therapy using boronophenylalanine for high-grade gliomas: part I.** *Clin Cancer Res* 1998, **4**:1825–1832.
12. Imahori Y, Ueda S, Ohmori Y, Sakae K, Kusuki T, Kobayashi T, Takagaki M, Ono K, Ido T, Fujii R: **Positron emission tomography-based boron neutron capture therapy using boronophenylalanine for high-grade gliomas: part II.** *Clin Cancer Res* 1998, **4**:1833–1841.
13. Miyashita M, Miyatake S, Imahori Y, Yokoyama K, Kawabata S, Kajimoto Y, Shibata MA, Otsuki Y, Kirihata M, Ono K, Kuroiwa T: **Evaluation of fluoride-labeled boronophenylalanine-PET imaging for the study of radiation effects in patients with glioblastomas.** *J Neurooncol* 2008, **89**:239–246.
14. Brandsma D, Stalpers L, Taal W, Sminia P, van den Bent MJ: **Clinical features, mechanisms, and management of pseudoprogression in malignant gliomas.** *Lancet Oncol* 2008, **9**:453–461.
15. Friedman HS, Prados MD, Wen PY, Mikkelsen T, Schiff D, Abrey LE, Yung WK, Paleologos N, Nicholas MK, Jensen R, *et al*: **Bevacizumab alone and in**

combination with irinotecan in recurrent glioblastoma. *J Clin Oncol* 2009, 27:4733–4740.
16. Vredenburgh JJ, Desjardins A, Herndon JE 2nd, Marcello J, Reardon DA, Quinn JA, Rich JN, Sathornsumetee S, Gururangan S, Sampson J, *et al*: Bevacizumab plus irinotecan in recurrent glioblastoma multiforme. *J Clin Oncol* 2007, 25:4722–4729.
17. Gutin PH, Iwamoto FM, Beal K, Mohile NA, Karimi S, Hou BL, Lymberis S, Yamada Y, Chang J, Abrey LE: Safety and efficacy of bevacizumab with hypofractionated stereotactic irradiation for recurrent malignant gliomas. *Int J Radiat Oncol Biol Phys* 2009, 75:156–163.
18. Niyazi M, Ganswindt U, Schwarz SB, Kreth FW, Tonn JC, Geisler J, la Fougere C, Ertl L, Linn J, Siefert A, Belka C: Irradiation and bevacizumab in high-grade glioma retreatment settings. *Int J Radiat Oncol Biol Phys* 2012, 82:67–76.
19. Torcuator RG, Thind R, Patel M, Mohan YS, Anderson J, Doyle T, Ryu S, Jain R, Schultz L, Rosenblum M, Mikkelsen T: The role of salvage reirradiation for malignant gliomas that progress on bevacizumab. *J Neurooncol* 2010, 97:401–407.

doi:10.1186/1748-717X-9-6
Cite this article as: Miyatake *et al.*: Boron neutron capture therapy with bevacizumab may prolong the survival of recurrent malignant glioma patients: four cases. *Radiation Oncology* 2014 9:6.

Journal of Radiation Research, 2014, 55, 75–83
doi: 10.1093/jrr/rrt095 Advance Access Publication 16 August 2013

High linear-energy-transfer radiation can overcome radioresistance of glioma stem-like cells to low linear-energy-transfer radiation

Yuki HIROTA[1], Shin-Ichiro MASUNAGA[2], Natsuko KONDO[2], Shinji KAWABATA[1], Hirokazu HIRAKAWA[3], Hirohiko YAJIMA[3], Akira FUJIMORI[3], Koji ONO[2], Toshihiko KUROIWA[1] and Shin-Ichi MIYATAKE[1,*]

[1]Department of Neurosurgery, Osaka Medical College, 2–7 Daigaku-machi, Takatsuki City, Osaka 569-8686, Japan
[2]Particle Radiation Oncology Research Center, Research Reactor Institute, Kyoto University, Osaka, Japan
[3]Cellular and Molecular Biology Team, National Institute of Radiological Science, Heavy-ion Radiobiology Research Group, Research Center for Charged Particle Therapy, Chiba, Japan
*Corresponding author: Department of Neurosurgery, Osaka Medical College, 2–7 Daigaku-machi, Takatsuki City, Osaka 569-8686, Japan. Tel: +81-72-683-1221; Fax: +81-72-681-3723; Email: neu070@poh.osaka-med.ac.jp

(Received 5 March 2013; revised 24 June 2013; accepted 26 June 2013)

Ionizing radiation is applied as the standard treatment for glioblastoma multiforme (GBM). However, radiotherapy remains merely palliative, not curative, because of the existence of glioma stem cells (GSCs), which are regarded as highly radioresistant to low linear-energy-transfer (LET) photons. Here we analyzed whether or not high-LET particles can overcome the radioresistance of GSCs. Glioma stem-like cells (GSLCs) were induced from the GBM cell line A172 in stem cell culture medium. The phenotypes of GSLCs and wild-type cells were confirmed using stem cell markers. These cells were irradiated with ^{60}Co gamma rays or reactor neutron beams. Under neutron-beam irradiation, high-LET proton particles can be produced through elastic scattering or nitrogen capture reaction. Radiosensitivity was assessed by a colony-forming assay, and the DNA double-strand breaks (DSBs) were assessed by a histone gamma-H2AX focus detection assay. In stem cell culture medium, GSLCs could form neurosphere-like cells and express neural stem cell markers (Sox2 and Musashi) abundantly in comparison with their parental cells. GSLCs were significantly more radioresistant to gamma rays than their parental cells, but neutron beams overcame this resistance. There were significantly fewer gamma-H2AX foci in the A172 GSLCs 24 h after irradiation with gamma rays than in their parental cultured cells, while there was no apparent difference following neutron-beam irradiation. High-LET radiation can overcome the radioresistance of GSLCs by producing unrepairable DNA DSBs. High-LET radiation therapy might have the potential to overcome GBM's resistance to X-rays in a clinical setting.

Keywords: glioblastoma multiforme; glioma stem cells; linear energy transfer; neutron beams; gamma rays

INTRODUCTION

Radiation therapy with surgery and chemotherapy is the standard treatment for glioblastoma multiforme (GBM) [1]. However, the prognosis of patients with GBM has not improved in recent decades, and almost half of GBM patients do not survive the first year after diagnosis. Thus, another, more promising therapy for GBM is needed. Recently, some reports have shown the presence of glioma stem cells (GSCs) in malignant gliomas [2–4]. These cells are highly resistant to radiotherapy because of their enhanced checkpoint response to radiation [5]. Other studies have shown that GSCs express high levels of sirtuin family genes (especially the SirT1 gene) and that these upregulations are relevant to radiosensitivity because they modulate apoptotic activity in response to irradiation to GSCs [6]. As a result, GSCs are now known to play important roles in tumor progression and relapse after radiotherapy and chemotherapy, and new therapeutic strategies targeting GSCs should be developed to treat patients with GBM. In the previous reports, radioresistance of GSCs was studied in a subpopulation with a specific phenotype. In these studies, it was difficult to use appropriate control cells for the GSCs. Therefore, we induced glioma stem-like cells (GSLCs) in which the phenotypes of GSCs

were enriched, and used the wild-type GBM cells as controls in this study.

On the other hand, we have applied boron neutron capture therapy (BNCT) for malignant brain tumors, including GBM [7–9]. This is a unique tumor-selective particle radiotherapy using neutron irradiation, especially thermal neutron irradiation. Boron-10 (^{10}B) releases alpha (^{4}He) and ^{7}Li particles through ^{10}B (n,α)^{7}Li reaction. The key players in the anti-tumor effects of BNCT are these high linear-energy-transfer (LET) particles. With BNCT, good results have already been achieved for patients with newly diagnosed GBM and recurrent malignant glioma [9, 10], although the numbers of such cases in clinical trials have been limited.

So far, the radioresistance of GSCs has been examined mainly in terms of low-LET radiation such as X-rays or gamma rays. Therefore, we hypothesized that high-LET radiation could overcome the radioresistance of GSCs. In fact, a previous study showed that high-LET radiation was more effective than low-LET radiation for promoting DNA damage [11]. Here, we employed a reactor neutron-beam irradiation system that produces high-LET proton particles through elastic scattering and nitrogen capture reaction. We analyzed the usefulness of high-LET radiation for overcoming the radioresistance to low-LET radiation in GSCs using GSLCs, as well as the ability of these cells to recover from radiation-induced DNA damage by a gamma-H2AX assay.

MATERIALS AND METHODS

Cell culture

The human GBM cell line A172 was purchased from American Type Culture Collection (Manassas, VA) and cultured in Dulbecco's modified Eagle's medium (DMEM; Invitrogen, Carlsbad, CA) with 10% fetal bovine serum (FBS) with penicillin and streptomycin at 37°C in an atmosphere of 5% CO_2. GSLCs were induced from A172 cells in serum-free medium (SFM) as described previously [12]. The SFM was composed of DMEM/F12 (Sigma-Aldrich, St Louis, MO), 20 ng/ml basic fibroblast growth factor (Peprotech, Rocky Hill, NJ), 20 ng/ml epidermal growth factor (Peprotech), 2 μg/ml heparin (Sigma-Aldrich), and B27 supplement (50×; Life Technology/Invitrogen).

Western blot analysis

Cells were cultured for 7 d in each culture medium. Protein samples were prepared with 10% sodium dodecyl sulfate-polyacrylamide gel electrophoresis and transferred onto nitrocellulose membranes. Immune complexes were formed by incubation with the stem cell markers CD133 (Cell Signal Technology, Danvers, MA), Sox2 (Cell Signal Technology), and Musashi (Cell Signal Technology) overnight at 4°C. As a control for the housekeeping gene products, Ku70 (Thermo Scientific, Waltham, MA) was employed. Blots were washed and incubated for 1 h with horseradish peroxidase-conjugated anti-mouse and anti-rabbit secondary antibodies (Santa Cruz Biotechnology, Santa Cruz, CA). Immunoreactive protein bands were detected by using an enhanced chemoluminescence Advance Western Blotting Detection Kit (GE Health Care, Buckinghamshire, UK), and Image Reader LAS-1000 Pro ver. 2.5 (Fuji Photo Film, Tokyo, Japan).

Fluorescence-activated cell sorting analysis

Cells were cultured for 7–14 d in each culture medium. Cells were collected and incubated with anti-CD133 antibody (Bioss, Woburn, MA) for 1 h at 37°C. After washing, the cells were incubated with Alexa Fluor 647-labeled anti-rabbit secondary antibody for 30 min at 37°C, then analyzed by fluorescence-activated cell sorting (FACS) using a BD FACS Aria Cell Sorter (BD Bioscience, San Jose, CA).

Gamma-ray and neutron-beam irradiation

Two sets of A172 cells, one cultured with serum-containing medium (DMEM + 10% FBS) and the other cultured with SFM, were trypsinized, and single-cell suspensions were placed into a Teflon tube and irradiated at room temperature by neutron beams or gamma rays.

At the Heavy Water Column of the Kyoto University Research Reactor (KUR), neutron-beam irradiation was performed at a power of 1 MW. The neutron fluence was measured from the radioactivation of gold foil. Contaminating gamma rays, including secondary gamma rays, were measured with thermoluminescence dosimeter (TLD) powder. The TLD used was beryllium oxide (BeO) enclosed in a quartz glass capsule. BeO itself is sensitive to thermal neutrons [13]. The average neutron fluxes were 1.0×10^{9} n/cm^2/s for the thermal neutron range (less than 0.6 keV), 1.6×10^{8} n/cm^2/s for the epithermal neutron range (0.6–10 keV), and 9.4×10^{6} n/cm^2/s for the fast neutron range (more than 10 keV). The total absorbed doses resulting from fast, epithermal, and thermal neutron-beam irradiation were calculated as the sum of the absorbed doses attributed primarily to ^{1}H(n,n)^{1}H, ^{14}N(n,p)^{14}C, and contaminating gamma rays. The dose-converting coefficients and details of the calculation method have been described previously [14, 15].

Gamma-ray irradiation was applied using a ^{60}Co gamma-ray irradiator at a dose rate of 1.3 Gy/min.

Colony-forming assay

Cell survival was defined using a colony-forming assay. The irradiated cells were seeded into 100 mm dishes at various densities depending on the physical dose that cells received, and cultured in a serum-containing medium. After 13–15 d, the colonies were stained with methylene blue. A cell cluster containing at least 50 cells was considered a single colony. The surviving fraction was calculated as the number of colonies of treated cells divided by that for the control cells. The D_{10} values were derived by linear quadratic model analysis